A new insight into the growth mode of metals on TiO_2(110)

Minghui Hu *, Suguru Noda, and Hiroshi Komiyama

Department of Chemical System Engineering, University of Tokyo

7-3-1 Hongo, Bunkyo-ku, Tokyo 113-8656, Japan

phone: +81-3-5841-7330, fax: +81-3-5841-7230, e-mail: mhu@chemsys.t.u-tokyo.ac.jp

Abstract

The growth of metals on TiO_2(110) at one monolayer coverage is classified into three-dimensional island, two-dimensional layer, and transition growth zones via two thermodynamic parameters, the heat of formation of metal oxides, $-\Delta_f H^0_{\text{oxide of M}}$, and the heat of sublimation of metals, $-\Delta_f H^0_{\text{metal, per mol of metal}}$ (both expressed per mol of metal), which are easily obtainable. These two parameters represent the strength of metal/TiO_2(110) interfacial interactions and the strength of metal/metal lateral interactions, respectively. Such classification is based on the thermodynamic criteria that the growth mode of metals on TiO_2(110) is determined by metal/TiO_2 interfacial free energy and metal surface free energy. Compared with the conventional approach that only uses the heat of formation of metal oxides, $-\Delta_f H^0_{\text{oxide of O}}$ (expressed per mol of oxygen), our model provides a clearer and more comprehensive vision of the growth mode of metals on TiO_2(110) and the factors affecting the growth mode. The approach described in this study can also be applied to other metal/reducible oxide systems.

Keywords: Growth; Single crystal surfaces; Titanium oxide; Metallic films; Surface chemical reaction; Wetting.

1. Introduction

An understanding of the growth mode of metals on oxide surfaces is important for the design of electronic devices, catalysts, and sensors. If there are no specific adsorption sites on substrate surfaces and the desorption of adatoms is negligible, the initial thin-film growth process can be simplified as follows. Atoms arrive at and are adsorbed on substrate surfaces at a rate determined by the deposition flux. As one adatom diffuses over substrate surfaces, it either collides with another adatom and forms a new, immobile cluster, or collides with and is captured by an existing cluster. If the inter-cluster distance is larger than the surface diffusion length, new clusters will be formed on empty areas between existing clusters. In this way, kinetics determines the structure of total clusters, such as inter-cluster distance and number density. On the other hand, the size of clusters in most cases is small enough compared with the surface diffusion length, except for those depositions at low temperature or at a high deposition flux. This results in that individual clusters are structurally relaxed. Therefore, the geometry of individual clusters, i.e., the growth mode, usually only depends on thermodynamics.

Rutile TiO_2 is a typical transition metal oxide used in such applications. In the 1990's, the growth mode of metals on TiO_2(110) was actively studied and summarized [1, 2]. Whether metals grow in the two-dimensional (2D) layer (Frank-van-der-Merve) mode or in the three-dimensional (3D) island (Volmer-Weber) mode, is closely related to the strength of metal/TiO_2 interfacial interactions, which is represented by interfacial oxidation/reduction

reactions between metals and TiO_2.

In spite of the existing understanding of the nucleation and growth mechanisms of metals on TiO_2(110), a clear and comprehensive vision of the growth mode and the factors that might affect the growth mode has never been given. Therefore, it is the purpose of this study to provide such a vision from the viewpoint of thermodynamics. In our model, we use the heat of formation of metal oxides and the heat of sublimation of metals (both expressed per mol of metal) to classify the growth mode at one monolayer (ML) coverage into 3D island, 2D layer, and transition growth zones. These two parameters correspond to the strength of metal/TiO_2 interfacial interactions and the strength of metal/metal lateral interactions, respectively. Such a thermodynamics-based approach is not only valid for describing the growth of metals on TiO_2(110), but also applicable to other metal/reducible oxide systems.

2. Review of previous work on the growth mode of metals on TiO_2(110)

The (110) facet is the most stable surface for rutile TiO_2 [3]. Depending on formation conditions, TiO_2(110) surfaces show unreconstructed stoichiometric 1×1 and more complex non-stoichiometric 1×n (n = 1-4) phases [4]. Figure 1 shows the structure of 1×1 phase depicted as a bridging-oxygen row model [5], whereas the structures of 1×n phases are still not well understood [6-11]. Nevertheless, on the top surface of any phase, oxygen anions predominately exist, and titanium cations are potentially reducible by deposited metal atoms. Thus, by neglecting other interfacial interactions such as metal/Ti interactions and interfacial stress, metal/TiO_2 interfacial interactions can be approximately represented by interfacial reduction/oxidation reactions between metals and TiO_2 [2, 12]. Moreover, the high diffusivity of oxygen through TiO_2 lattices (d = 2.77×10^{-11} m^2/s at 348K) [13] may cause these charge-transfer reactions to occur at interfaces to a depth of several MLs [14-16].

Various metals have been deposited on TiO_2(110), and their growth modes are summarized in Table 1 [1, 12, 14-52]. Here, the growth mode is strictly defined at one ML coverage due to the ambiguity of experimental data for multilayer coverage. As explained in the introduction section, because most of these depositions are carried out at room temperature and at a low deposition flux, it is reasonable to suppose that the growth mode only depends on thermodynamics.

According to Bauer's criterion [53], the growth mode under thermodynamic equilibrium conditions is determined by the following parameters:

$$\Delta\gamma = \gamma_{metal} + \gamma_{metal-substrate} - \gamma_{substrate} \quad (1)$$

where γ_{metal}, $\gamma_{metal\text{-}substrate}$, and $\gamma_{substrate}$ (J/m^2) are the free energies of metal surfaces, metal/TiO_2 interfaces, and TiO_2(110) substrate surfaces, respectively. For $\Delta\gamma > 0$, 3D island growth occurs; otherwise, 2D layer growth occurs. Surface free energies of most metals (0.1-4.0 J/m^2) [54] are usually higher than that of TiO_2(110) (0.3-0.4 J/m^2) [55]. As a result, 3D island growth is thermodynamically favorable unless strong interfacial reduction/oxidation reactions cause a large, negative value of $\gamma_{metal\text{-}substrate}$ [56]. Because of the difficulty to directly measure $\gamma_{metal\text{-}substrate}$, some approximate estimations of $\gamma_{metal\text{-}substrate}$ must be considered. If interfacial interactions other than reduction/oxidation reactions are negligible, such as metal/Ti interactions and interfacial stress, the heat of formation of metal oxides formed at metal/TiO_2 interfaces per unit area, $-\Delta_f H^0_{\text{oxide of unit area}}$ (kJ/m^2), can be used to approximate $\gamma_{metal\text{-}substrate}$ [57]. Furthermore, by neglecting the actual electronic state and structural geometry of metal oxides formed at metal/TiO_2(110) interfaces, $-\Delta_f H^0_{\text{oxide of unit area}}$ can be further simplified into the heat of formation of the most stable metal oxides either expressed per mol of oxygen, $-\Delta_f H^0_{\text{oxide of O}}$ (kJ per mol of oxygen), or expressed per mol of metal, $-\Delta_f H^0_{\text{oxide of M}}$ (kJ per mol of metal). Both $-\Delta_f H^0_{\text{oxide of O}}$ and $-\Delta_f H^0_{\text{oxide of M}}$ approximately represent the strength of metal/TiO_2(110) interfacial interactions, i.e., $\gamma_{metal\text{-}substrate}$. Figure 2 shows the conventional

description of the growth mode of metals on TiO_2(110) by using either $-\Delta_fH^0_{\text{oxide of O}}$ or $-\Delta_fH^0_{\text{oxide of M}}$. Both $-\Delta_fH^0_{\text{oxide of O}}$ and $-\Delta_fH^0_{\text{oxide of M}}$ data used in Fig. 2 are experimental values obtained from Ref. [58]. Seen from the distribution of 3D island and 2D layer growth, $-\Delta_fH^0_{\text{oxide of O}}$ [Fig. 2(a)] correlates better with the growth mode than $-\Delta_fH^0_{\text{oxide of M}}$ [Fig. 2(b)]. As shown in Fig. 2(a), metals with a large $-\Delta_fH^0_{\text{oxide of O}}$, such as alkali, alkaline earth, and early-to-mid transition metals, tend to wet on TiO_2(110) and grow in the 2D layer mode, whereas metals with a small or negative $-\Delta_fH^0_{\text{oxide of O}}$, such as mid-to-late transition metals, tend to agglomerate into 3D islands, even at very low surface coverage.

Although $-\Delta_fH^0_{\text{oxide of O}}$ can explain the tendency of the growth-mode variation, for $200 < -\Delta_fH^0_{\text{oxide of O}} < 400$ kJ per mol of oxygen, the dominant growth mode remains ambiguous. Moreover, only from the viewpoint of metal/TiO_2(110) interfacial interactions, some nucleation and growth features can not be well explained and predicted. For example, the appearance of 3D islands 2ML high for Cr [24, 25] and V [50, 51] can not be well explained, nor can the different dependence of the growth mode on temperature for Fe [12] and Cu [29] be well explained.

3. New approach to the growth mode of metals on TiO_2(110)

The discussion about the conventional approach to describing the growth mode of metals on TiO_2(110) suggests that only using $-\Delta_fH^0_{\text{oxide of O}}$ that approximately represents the strength of metal/TiO_2 interfacial interactions, i.e., $\gamma_{\text{metal-substrate}}$, is not sufficient to determine the growth mode of metals on TiO_2(110). An additional thermodynamic parameter, γ_{metal}, which reflects the strength of metal/metal lateral interactions, must also be considered.

Most room-temperature γ_{metal} data originate either from liquid-phase surface tension measurements extrapolated to room temperature [59] or from theoretical calculations [54, 60],

whose reliability and accuracy remain unclear. The heat of sublimation per mol of metals, $-\Delta_f H^0_{\text{metal, per mol of metal}}$ (kJ/mol), or per unit surface, $-\Delta_f H^0_{\text{metal, per unit surface}}$ (kJ/m^2) can be used as the parameter instead of γ_{metal}, because both $-\Delta_f H^0_{\text{metal, per mol of metal}}$ and $-\Delta_f H^0_{\text{metal, per unit surface}}$ represent the strength of metal/metal lateral interactions and can be related by the following expressions [55, 61, 62]:

$$\gamma^{i}_{metal} = \frac{\sqrt{z^{b}} - \sqrt{z^{1}}}{\sqrt{z^{b}}} \times \Delta^{i}_{f} H^{0}_{\text{metal, per unit area}} \tag{2}$$

$$\Delta_f H^{0}_{\text{metal, per unit area}} = \frac{\Delta_f H^{0}_{\text{metal, per mol of metal}}}{N_A} \times f \times \left(\frac{\rho_{metal} \times N_A}{M_{metal}} \right)^{2/3} \tag{3}$$

where *i* refers to a specific facet of metal crystals, *z* is the coordination number, *b* refers to the bulk, *1* refers to the first surface layer, *f* represents the crystal geometry factor (≈1), N_A is Avogadro's constant, ρ_{metal} is the metal density (kg/m^3), and M_{metal} is the atomic weight (kg/mol). γ^{i}_{metal} and $-\Delta^{i}_{f}H^{0}_{\text{metal, per unit area}}$ depend on the specific facet of metal crystals, whereas $-\Delta_f H^0_{\text{metal, per unit area}}$ and $-\Delta_f H^0_{\text{metal, per mol of metal}}$ are average values. Neglecting the geometry of a particular crystalline facet and only considering average values, $-\Delta_f H^0_{\text{metal, per mol of metal}}$ is an appropriate approximation of γ_{metal}, because $-\Delta_f H^0_{\text{metal, per mol of metal}}$ is a parameter that can be directly obtained from thermodynamic handbooks and at the same time correlates well with experimental values of γ_{metal} as shown in Fig. 3. γ_{metal} and $-\Delta_f H^0_{\text{metal, per mol of metal}}$ data used in Fig. 3 are experimental values obtained from Refs. [59] and [58], respectively.

Figure 4 shows the description of the growth mode of metals on TiO_2(110) using $-\Delta_f H^0_{\text{metal, per mol of metal}}$ and either $-\Delta_f H^0_{\text{oxide of O}}$ or $-\Delta_f H^0_{\text{oxide of M}}$. Seen from the distribution of 3D island and 2D layer growth, $-\Delta_f H^0_{\text{oxide of M}}$ [Fig. 4(b)] correlates better with the growth mode than $-\Delta_f H^0_{\text{oxide of O}}$ [Fig. 4(a)]. In Fig. [4(b)], a line with a slope of $-\Delta_f H^0_{\text{metal, per mol of metal}} / -\Delta_f H^0_{\text{oxide of M}} = 1$ divides the diagram into three zones: 3D island (*Zone I*), 2D layer (*Zone II*), and transition growth (*Zone III*). In *Zone I*, $-\Delta_f H^0_{\text{metal, per mol of metal}} / -\Delta_f H^0_{\text{oxide of M}} > 1$, which means

metal/metal lateral interactions are stronger than metal/TiO_2 interfacial interactions. Therefore, metals in *Zone I* tend to grow in the 3D island mode dominated by metal/metal lateral interactions. On the contrary, in *Zone III*, $-\Delta_f H^0_{\text{metal, per mol of metal}} / -\Delta_f H^0_{\text{oxide of M}} < 1$, which means metal/metal lateral interactions are weaker than metal/TiO_2 interfacial interactions. Therefore, metals in *Zone III* tend to grow in the 2D layer mode dominated by metal/TiO_2 interfacial interactions. Between these two areas there is a transition area (*Zone II*) where $-\Delta_f H^0_{\text{metal, per mol of metal}} / -\Delta_f H^0_{\text{oxide of M}} \approx 1$, which implies that the strength of metal/metal lateral interactions is comparable to that of metal/TiO_2 interfacial interactions. As a result, metals in *Zone II* show either 3D island or 2D layer growth, depending on factors other than $-\Delta_f H^0_{\text{metal, per mol of metal}} / -\Delta_f H^0_{\text{oxide of M}}$. These factors contain weakened reducibility of TiO_2(110) surfaces, interfacial stress induced by lattice mismatch, and kinetic constraints such as temperature and surface roughness. As a result, some specific growth features frequently appear in *Zone II*. For example, Cr shows a so-called quasi-2D growth on TiO_2(110) [24, 25]. As the surface coverage increases up to 0.8 ML, due to the saturation of the reducibility of TiO_2(110) surfaces, additional incoming Cr atoms grow on the 2D layers to form 3D islands 2ML high. Similarly, V as a metal adjacent to Cr in *Zone II* also shows this quasi-2D growth behavior [50, 51]. In addition, the mismatch-dependent interfacial stress also contributes to the growth mode of some bcc metals (Nb, Cr, Fe, and V) in *Zone II* showing the epitaxial relationship of (100)[001] metal || (110)[001] TiO_2 [39, 52, 63]. Nb overlayers grow in the 2D layer mode and show a long-range order due to the small lattice mismatch (1%) along the [110] direction of TiO_2(110) [39]. On the contrary, Cr, Fe and V overlayers grow in the 3D island mode and lack the long-range order due to relatively large lattice mismatches of -13%, -13%, and -7%, respectively, along the [110] direction of TiO_2(110) [39, 52, 63]. Moreover, kinetics-limited growth can be observed for metals in *Zone II*. Fe grows in the 3D island mode at 300 K, but it grows in the 2D layer mode at 160 K [12]. When the temperature is decreased far below room

temperature, the surface diffusion length of Fe adatoms might be as small as the scale of atomic bond length, so that Fe adatoms reach equilibrium only within that small scale. In other words, Fe adatoms are absorbed and frozen immediately on TiO_2(110) surface where they arrive. Thus, kinetics-limited 2D layer growth appears due to the lowered mobility of Fe adatoms at low temperature. The increased surface roughness of TiO_2(110) also lowers the mobility of Fe adatoms, which changes the growth mode from 3D island to 2D layer [31]. Most metals in *Zones I* and *III* do not show such kinetics-limited features: Cu in *Zone I* grows in the 3D island mode at both 300 and 160 K [24], and Cs in *Zone III* grows in the 2D layer mode at both 300 and 130 K [26]. These factors, although usually negligible for typical 3D island growth shown in *Zone I* or 2D layer growth shown in *Zone III*, play an important role in this transition zone.

Comparing Fig. 4(a) with Fig. 4(b) indicates that in our model, $-\Delta_f H^0_{\text{oxide of M}}$ correlates better with the growth mode than $-\Delta_f H^0_{\text{oxide of O}}$, whereas in the conventional model, $-\Delta_f H^0_{\text{oxide of O}}$ correlates better with the growth mode than $-\Delta_f H^0_{\text{oxide of M}}$. This contradiction leads to a question: when describing the growth mode of metals on TiO_2(110), which parameter is thermodynamically more appropriate to be used as the substitution for $\gamma_{\text{metal-substrate}}$? Figure 5 shows the growth process of metals on TiO_2 below one ML coverage. Depending on the differences in metal-metal and metal-oxygen binding strengths, incoming metal atoms preferentially attach either to metal adatoms on TiO_2 surfaces or to oxygen anions of TiO_2 surfaces. If metal-metal binding is stronger than metal-oxygen binding, incoming metal atoms thermodynamically favor combination with metal adatoms, resulting in 3D island growth. Otherwise, they thermodynamically favor combination with oxygen anions of TiO_2, resulting in 2D layer growth. Therefore, the growth mode can be considered to result from the competition of metal adatoms with oxygen anions for incoming metal atoms. This competition depends on the binding strength expressed per incoming metal atom, but not on

the binding strength expressed per oxygen anion. Moreover, $-\Delta_f H^0_{\text{oxide of M}}$ has the same unit as $-\Delta_f H^0_{\text{metal, per mol of metal}}$, kJ per mol of metal. It is therefore reasonable that the strength of metal/metal lateral interactions is comparable to that of metal/TiO_2 interfacial interactions when $-\Delta_f H^0_{\text{metal, per mol of metal}} / -\Delta_f H^0_{\text{oxide of M}} \approx 1$. Therefore, $-\Delta_f H^0_{\text{oxide of M}}$ is more appropriate than $-\Delta_f H^0_{\text{oxide of O}}$ in our thermodynamics-based classification of the growth mode of metals on TiO_2(110).

As described before, according to Bauer's criterion, the growth mode of metals on TiO_2(110) is related to three factors, γ_{metal}, $\gamma_{\text{metal-substrate}}$, and $\gamma_{\text{substrate}}$. Among them, $\gamma_{\text{substrate}}$ is the surface free energy of TiO_2(110), which is constant. Then, the growth mode should be determined by the remaining two variable parameters, γ_{metal} and $\gamma_{\text{metal-substrate}}$. In our model, we substitute γ_{metal} and $\gamma_{\text{metal-substrate}}$ with two simple thermodynamic parameters, $-\Delta_f H^0_{\text{metal, per mol of metal}}$ and $-\Delta_f H^0_{\text{oxide of M}}$, respectively. This approach successfully describes the growth mode of metals on TiO_2(110) and the factors affecting the growth mode. Our model can be further improved by considering actual metal oxides formed at metal/TiO_2 interfaces and other factors. Nevertheless, it agrees well with available experimental results regarding the growth mode of metals on TiO_2(110), and the model parameters can be easily obtained from thermodynamic handbooks. Our model not only provides a thermodynamic explanation for experimental results, but for the first time, it also permits prediction of the growth mode of other metals on TiO_2(110) in advance. This approach should also be applicable to other metal/reducible oxide systems in which the characteristics of interfacial interactions are primarily considered as interfacial oxidation/reduction reactions.

4. Conclusions

The growth mode of metals on TiO_2(110) at one monolayer (ML) coverage is classified

into 3D island (*I*), 2D layer (*III*), and transition growth (*II*) zones via two easily obtainable thermodynamic parameters, $-\Delta_f H^0_{\text{oxide of M}}$ and $-\Delta_f H^0_{\text{metal, per mol of metal}}$, which represent the strength of metal/TiO_2(110) interfacial interactions and the strength of metal/metal lateral interactions, respectively. When $-\Delta_f H^0_{\text{metal, per mol of metal}} / -\Delta_f H^0_{\text{oxide of M}} > 1$ (*Zone I*), metals show 3D island growth dominated by metal/metal lateral interactions. On the contrary, when $-\Delta_f H^0_{\text{metal, per mol of metal}} / -\Delta_f H^0_{\text{oxide of M}} < 1$ (*Zone III*), metals show 2D island growth dominated by metal/TiO_2 interfacial interactions. Between these two zones there is a transition zone (*Zone II*) where $-\Delta_f H^0_{\text{metal, per mol of metal}} / -\Delta_f H^0_{\text{oxide of M}} \approx 1$, which implies that the strength of metal/metal lateral interactions is comparable to that of metal/TiO_2 interfacial reactions. As a result, metals in *Zone II* show either 3D island or 2D layer growth, depending other factors including weakened reducibility of TiO_2(110) surfaces, interfacial stress, and kinetic constraints.

Compared with the conventional approach to describing the growth mode of metals on TiO_2(110 via a single parameter, $-\Delta_f H^0_{\text{oxide of O}}$, our thermodynamics-based classification of the growth mode not only provides a clearer and more comprehensive vision of the growth mode of metals on TiO_2(110) and the factors affecting the growth mode, but also can be applied to other metal/reducible oxide systems.

Acknowledgments

The authors thank Professors Tatsuya Okubo and Yukio Yamaguchi of the University of Tokyo for helpful discussions and suggestions.

References

[1] U. Diebold, J.-M. Pan, and T. E. Madey, Surf. Sci. 331-333 (1995) 845.

[2] C. T. Campbell, Surf. Sci. Rep. 27 (1997) 1.

[3] M. Ramamoorthy, D. Vanderbilt, and R. D. King-Smith, Phys. Rev. B 49 (1994) 16721.

[4] E. Asari and R. Souda, Nucl. Instrum. Meth. B 161-163 (2000) 396.

[5] G. Charlton et al., Phys. Rev. Lett. 78 (1997) 495.

[6] P. J. Moller and M.-C. Wu, Surf. Sci. 224 (1989) 265.

[7] H. Onishi and Y. Iwasawa, Surf. Sci. Lett. 313 (1994) L783.

[8] S. Fischer, A. W. Munz, K. Schierbaum, and W. Gopel, Surf. Sci. 337 (1995) 17.

[9] K. Fukui, H. Onishi, and Y. Iwasawa, Phys. Rev. Lett. 79 (1997) 4202.

[10] C. L. Pang, H. Raza, S. A. Haycock, and G. Thornton, Appl. Surf. Sci. 157 (2000) 233.

[11] Y. Liang, S. Gan, S. A. Chambers, and E. I. Altman, Phys. Rev. B 63 (2001) 235402.

[12] J.-M. Pan and T. E. Madey, J. Vac. Sci. Technol. A 11 (1993) 1667.

[13] G. Rocker and W. Gopel, Surf. Sci. 181 (1987) 530.

[14] R. J. Lad and L. S. Dake, Mater. Res. Soc. Symp. Proc. 238 (1992) 823.

[15] L. S. Dake and R. J. Lad, Surf. Sci. 289 (1993) 297.

[16] B. Domenichini, S. Petigny, V. Blondeau-Patissier, A. Steinbrunn, and S. Bourgeois, Surf. Sci. 468 (2000) 192.

[17] D. A. Chen, M. C. Bartelt, S. M. Seutter, and K. F. McCarty, Surf. Sci. 464 (2000) L708.

[18] X. Lai, T. P. S. Clair, M. Valden, and D. W. Goodman, Progress in Surf. Sci. 509 (1998) 25.

[19] K. Luo, T. P. S. Clair, X. Lai, and D. W. Goodman, J. Phys. Chem. B 104 (2000) 3050.

[20] X. Lai, C. Xu, and D. W. Goodmana, J. Vac. Sci. Technol. A 16 (1998) 2562.

[21] S. C. Parker, A. W. Grant, V. A. Bondzie, and C. T. Campbell, Surf. Sci. 441 (1999) 10.

[22] N. Spiridis, J. Haber, and J. Korecki, Vacuum 63 (2001) 99.

[23] Z. Li, J. H. Jorgensen, P. J. Moller, M. Sambi, and G. Granozzi, Appl. Surf. Sci. 142 (1999) 135.

[24] U. Diebold, J.-M. Pan, and T. E. Madey, Surf. Sci. 287-288 (1993) 896.

[25] J.-M. Pan, U. Diebold, L. Z. Zhang, and T. E. Madey, Surf. Sci. 295 (1993) 411.

[26] M. Brause, S. Skordas, and V. Kempter, Surf. Sci. 445 (2000) 224.

[27] A. W. Grant and C. T. Campbell, Phys. Rev. B 55 (1999) 1844.

[28] D. A. Chen, M. C. Bartelt, R. Q. Hwang, and K. F. McCarty, Surf. Sci. 450 (2000) 78.

[29] U. Diebold, J.-M. Pan, and T. E. Madey, Phys. Rev. B 47 (1993) 3868.

[30] J. E. Reddic, J. Zhou, and D. A. Chen, Surf. Sci. 494 (2001) L767.

[31] H. Mostefa-Sba, B. Domenichini, and S. Bourgeois, Surf. Sci. 437 (1999) 107.

[32] B. E. Hayden and G. P. Nicholson, Surf. Sci. 274 (1992) 277.

[33] A. Berko and F. Solymosi, Magy. Ken. Foly. 106 (2000) 7.

[34] A. Berko and F. Solymosi, Surf. Sci. 411 (1998) L900.

[35] A. Berko and F. Solymosi, J. Phys. Chem. B 114 (2000) 10215.

[36] S. Petigny, H. Mostefa-Sba, B. Domenichini, E. Lesniewska, A. Steinbrunn, and S. Bourgeois, Appl. Surf. Sci. 142 (1999) 114.

[37] J. Nerlov, S. Weichel, E. H. Pedersen, P. J. Moller, and S. V. Christensen, Surf. Sci. 371 (1997) 321.

[38] H. Onishi, T. Aruga, C. Egawa, and Y. Iwasawa, Surf. Sci. 199 (1988) 54.

[39] J. Marien, T. Wagner, G. Duscher, A. Koch, and M. Ruhle, Surf. Sci. 446 (2000) 219.

[40] S. Bourgeois, P. L. Seigneur, M. Perdereau, D. Chandesris, P. L. Fevre, and H. Magnan, Thin Solid Films 304 (1997) 267.

[41] H. Onishi, T. Aruga, C. Egawa, and Y. Iwasawa, Surf. Sci. 233 (1990) 261.

[42] R. E. Tanner, I. Goldfarb, M. R. Castell, and G. A. D. Briggs, Surf. Sci. 486 (2001) 167.

[43] M. J. J. Jak, C. Konstapela, A. Van Kreuningena, J. Verhoevena, and J. W. M. Frenkenb, Surf. Sci. 457 (2000) 295.

[44] P. Stone, R. A. Bennett, S. Poulston, and M. Bowker, Surf. Sci. 433 (1999) 501.

[45] C. Xu, X. Lai, G. W. Zajac, and D. W. Goodman, Phys. Rev. B 56 (1997) 13464.

[46] F. Pesty, H. Steinruck, and T. E. Madey, Surf. Sci. 339 (1995) 83.

[47] A. Berko, G. Menesi, and F. Solymosi, Surf. Sci. 372 (1997) 202.

[48] A. Berko, I. Ulrych, and K. C. Prince, J. Phys. Chem. B 102 (1998) 3379.

[49] A. Berko, J. Szoko, and F. Solymosi, Solid State Ionics 141-142 (2001) 197.

[50] J. Biener, J. Wang, and R. J. Madix, Surf. Sci. 442 (1999) 47.

[51] J. Biener, M. Baumer, J. Wang, and R. J. Madix, Surf. Sci. 450 (2000) 12.

[52] M. Sambi, E. Pin, G. Sangiovanni, L. Zaratin, G. Granozzi, and F. Parmigiani, Surf. Sci. 349 (1996) L169.

[53] E. Bauer, Z. Kristallogr 110 (1958) 423.

[54] L. Vitos, A. Ruban, H. Skriver, and J. Kollar, Surf. Sci. 411 (1998) 186.

[55] S. H. Overbury, P. A. Bertrand, and G. A. Somorjai, Chem. Rev. 75 (1975) 547.

[56] J. H. Van Der Merwe, Interf. Sci. 1 (1993) 77.

[57] C. H. F. Peden, K. B. Kidd, and N. D. Shinn, J. Vac. Sci. Technol. A 9 (1991) 1518.

[58] D. R. Lide (Ed.), CRC Handbook of Chemistry and Physics, 80th ed. (CRC Press, Boca Raton, Landon, New York, Washington DC, 1999).

[59] W. R. Tyson, Surf. Sci. 62 (1977) 267.

[60] S. G. Wang, E. K. Tian, and C. W. Lung, J. Phys. Chem. Solids 61 (2000) 1295.

[61] A. R. Miedema and J. W. F. Dorleijn, Surf. Sci. 95 (1980) 447.

[62] L. Z. Mezey and J. Giber, Jpn. J. Appl. Phys. 21 (1982) 1569.

[63] J.-M. Pan, B. L. Maschhoff, U. Diebold, and T. E. Madey, Surf. Sci. 291 (1993) 381.

Figure captions

Fig. 1. Structure of (1×1) phase of TiO_2(110) surface: (a) plan-view and (b) side-view.

Fig. 2. Description of the growth mode of metals on TiO_2(110) versus: (a) $-\Delta_f H^0_{\text{oxide of O}}$, and (b) $-\Delta_f H^0_{\text{oxide of M}}$. Negative values of $-\Delta_f H^0_{\text{oxide of O}}$ and $-\Delta_f H^0_{\text{oxide of M}}$ (Au and Pt) are approximated as zero. Both $-\Delta_f H^0_{\text{oxide of O}}$ and $-\Delta_f H^0_{\text{oxide of M}}$ data are experimental values obtained from Ref. [58].

Fig. 3. Surface free energy, γ_{metal} (J/m^2), versus heat of sublimation, $-\Delta_f H^0_{\text{metal, per mol of metal}}$ (kJ/mol), for various metals.γ_{metal} and $-\Delta_f H^0_{\text{metal, per mol of metal}}$ data are experimental values obtained from Refs. [59] and [58], respectively.

Fig. 4. Description of the growth mode of metals on TiO_2(110) versus: (a) $-\Delta_f H^0_{\text{oxide of O}}$ and $-\Delta_f H^0_{\text{metal, per mol of metal}}$, and (b) $-\Delta_f H^0_{\text{oxide of M}}$ and $-\Delta_f H^0_{\text{metal, per mol of metal}}$, in which ● and Δ represent experimentally observed 3D island and 2D layer growth modes, respectively; and × represents the positions of metals whose growth modes have not been determined. The negative values of $-\Delta_f H^0_{\text{oxide of O}}$ and $-\Delta_f H^0_{\text{oxide of M}}$ (Au and Pt) are approximated as zero.

Fig. 5. Dependence of the growth mode on the strength of metal/metal lateral interactions and the strength of metal/oxygen interfacial interactions, from the viewpoint of competition of metal adatoms with oxygen anions for incoming metal atoms.

Fig. 1

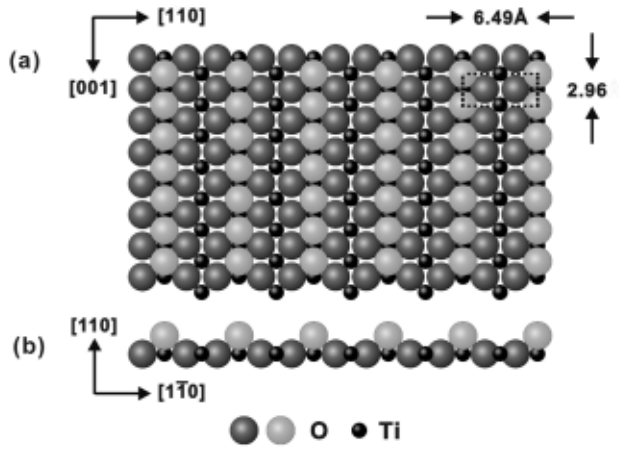

Fig. 2

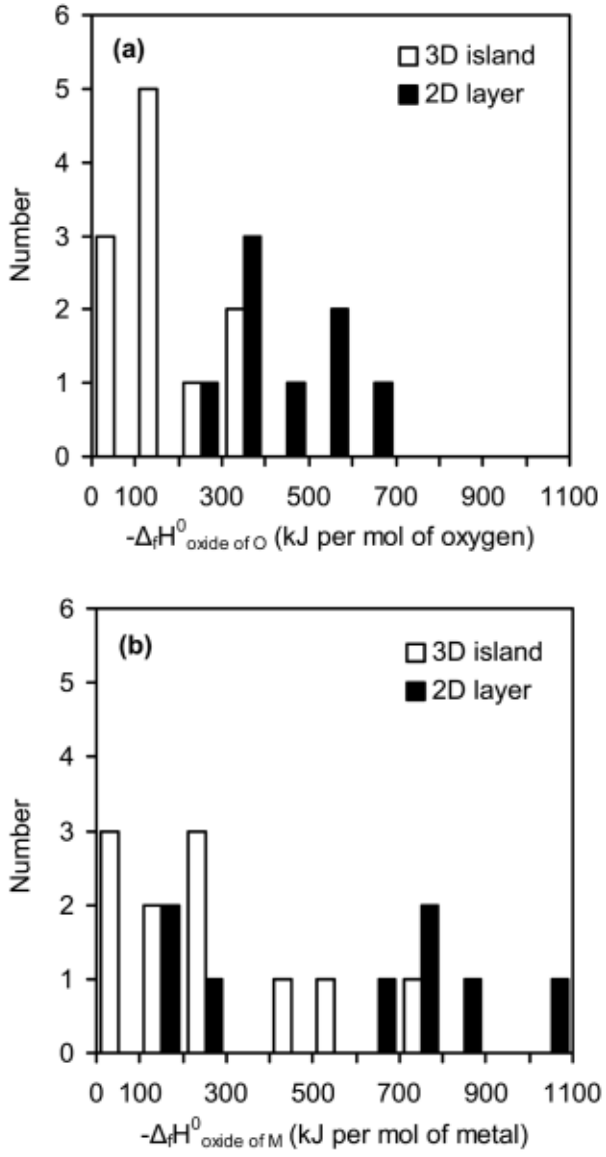
(a)
3D island
2D layer
Number
0
1
2
3
4
5
6
0 100 300 500 700 900 1100
$-\Delta_f H^0_{\text{oxide of O}}$ (kJ per mol of oxygen)
(b)
3D island
2D layer
Number
0
1
2
3
4
5
6
0 100 300 500 700 900 1100
$-\Delta_f H^0_{\text{oxide of M}}$ (kJ per mol of metal)

Fig. 3

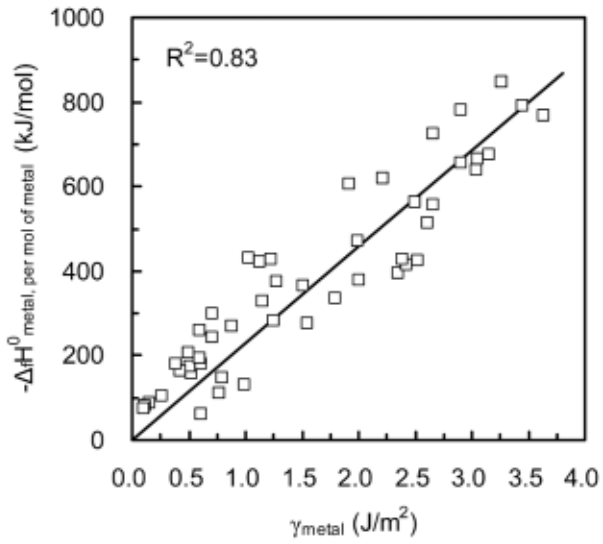
R^2=0.83
$-\Delta_f H^0_{metal,\ per\ mol\ of\ metal}$ (kJ/mol)
γ_{metal} (J/m^2)
0
200
400
600
800
1000
0.0
0.5
1.0
1.5
2.0
2.5
3.0
3.5
4.0

Fig. 4

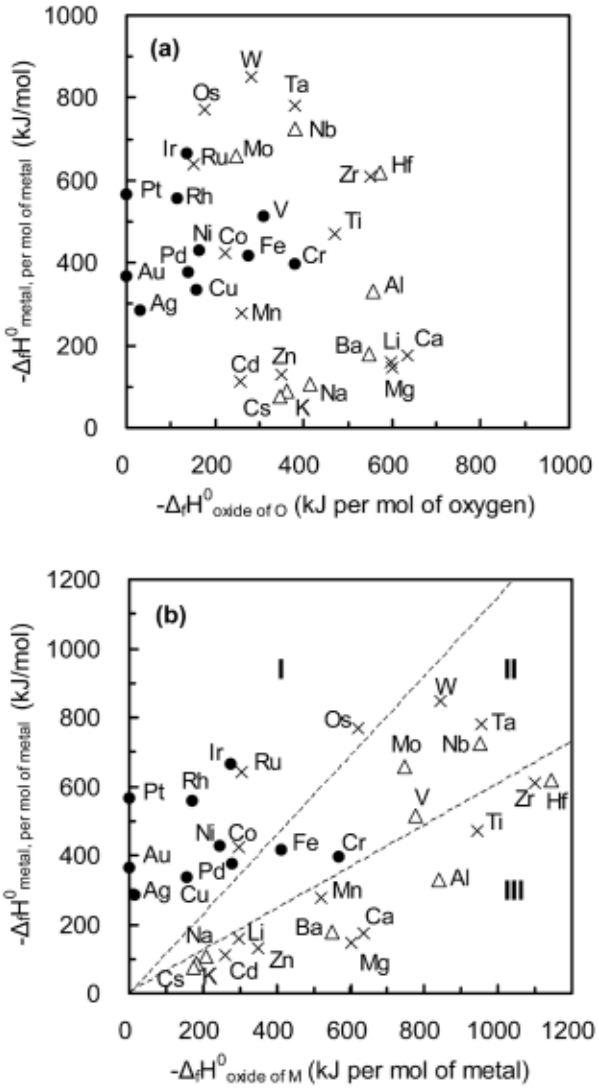
(a)
W
Os
Ta
Nb
Ir
Ru
Mo
Zr
Hf
Pt
Rh
V
Ti
Ni
Co
Fe
Cr
Pd
Au
Cu
Al
Ag
Mn
Ba
Li
Ca
Cd
Zn
Na
Mg
Cs
K
0
200
400
600
800
1000
$-\Delta_f H^0_{\text{metal, per mol of metal}}$ (kJ/mol)
$-\Delta_f H^0_{\text{oxide of O}}$ (kJ per mol of oxygen)
(b)
I
II
III
W
Os
Ta
Mo
Nb
Ir
Ru
Pt
Rh
V
Zr
Hf
Ti
Ni
Co
Fe
Cr
Au
Pd
Al
Ag
Cu
Mn
Ca
Ba
Na
Li
Zn
Mg
Cs
K
Cd
0
200
400
600
800
1000
1200
$-\Delta_f H^0_{\text{metal, per mol of metal}}$ (kJ/mol)
$-\Delta_f H^0_{\text{oxide of M}}$ (kJ per mol of metal)

Fig. 5

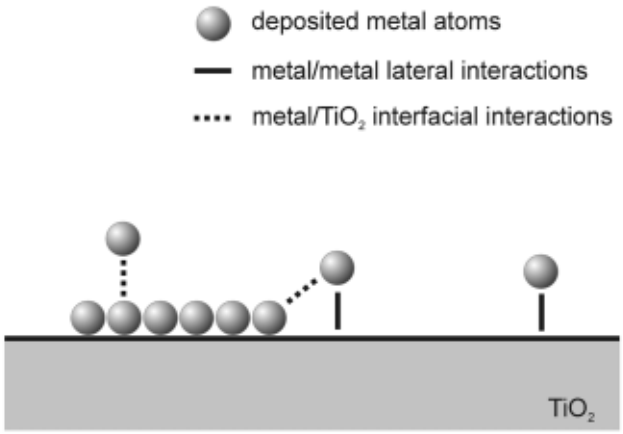
deposited metal atoms
metal/metal lateral interactions
metal/TiO2 interfacial interactions
TiO2